JOURNAL OF GEOPHYSICAL RESEARCH, VOL. 89, NO. B6, PAGES 4059-4071, JUNE 10, 1984

WATER IN MINERALS?
A PEAK IN THE INFRARED

Roger D. Aines and George R. Rossman

Division of Geological and Planetary Sciences California Institute of Technology

Abstract. The study of water in minerals with infrared spectroscopy is reviewed with emphasis on natural and synthetic quartz. Water can be recognized in minerals as fluid inclusions and as isolated molecules and can be distinguished from hydroxide ion. The distinction between very small inclusions and aggregates of structurally bound molecules is difficult. New studies of synthetic quartz using near-infrared spectroscopy are reported. These demonstrate that water molecules are the dominant hydrogen containing species in synthetic quartz but that this water is not in aggregates large enough to form ice when cooled.

Introduction

Hydrogen in minerals most frequently occurs bonded to oxygen. The resulting OH group is highly polar. Because this directed dipole is an efficient absorber of light in the infrared region, infrared spectroscopy is a powerful tool in the study of hydrogen in minerals.

In this paper we review the use of infrared spectroscopy (IR spectroscopy) with emphasis on the study of hydrogen in the silicate minerals and with a detailed examination of the hydrogen found in quartz. We also present new results regarding the spectrum of hydrogen in synthetic quartz. We distinguish two major categories of hydrogen in minerals: (1) stoichiometric hydrogen-bearing minerals, which contain hydrogen that is generally considered to be essential to the structure of the mineral and that appears explicitly in the chemical formula of the mineral and (2) trace hydrogen-bearing minerals which includes all cases where hydrogen can be detected in a mineral but where it is not essential to the structural identity of the mineral. Stoichiometric hydrogen occurs in gypsum as H_2O and in mica as OH^-. Examples of trace hydrogen include the hydrogen in cordierite (H_2O) and quartz (OH^-).

Minerals containing hydrogen, whether trace or stoichiometric, are commonly referred to as "hydrous" or "water bearing." This nomenclature reflects the fact that the neutral species H_2O is what is actually measured by common analytical techniques. We follow this convention when the speciation of the hydrogen is not known or we are referring to actual analytical measurements. The most important uses of IR spectroscopy in the study of hydrous minerals are (1) determining the actual speciation of hydrogen, (2) determining the crystallographic environment of that species, and (3) determining its analytical concentration.

Paper number 3B1062.
0148-0227/84/003B-1062$05.00

Identification of Hydrogen Species in Minerals

The most common species of hydrogen is H_2O. The spectrum of liquid H_2O is shown in Figures 1 and 2. The lower abscissa scale is in wavenumbers, a linear energy scale proportional to the frequency of the light exciting the absorption in units of cm^{-1}. The upper scale is a wavelength scale. The major features in Figure 1 are bands at 1630 wavenumbers and ~3400 wavenumbers. These are the fundamental absorptions of the molecule H_2O. The 1630-wavenumber absorption is due to the bending of the H_2O molecule, and the 3400-wavenumber band consists of a symmetric stretching absorption at 3220 wavenumbers and an antisymmetric stretching absorption at 3445 wavenumbers. The absorptions at higher wavenumbers in Figure 2 arise from linear combinations and multiples (overtones) of the fundamental vibrations. The spectral region below 4000 wavenumbers is referred to as the infrared (IR) and the region above 4000 wavenumbers is the near infrared (NIR). Absorption in the 3800 to 3000-wavenumber region is typical of the O-H stretching vibration, and its presence is the first indication that a mineral contains hydrogen.

Water in the crystalline environment, free of the extended hydrogen bonded networks typical of liquid water, can produce sharper absorptions than occur in the liquid water spectrum. Figure 3 is the spectrum of gypsum, $Ca_2SO_4 \cdot 2H_2O$. The two stretching modes near 3400 wavenumbers are well resolved from each other and are displaced from their position in liquid water. The bending modes near 1620 wavenumbers are proof that the molecule H_2O is present. They contain additional structure not found in the liquid water spectrum because of interactions between water molecules. The existence of water is further confirmed by the combination modes at ~1900 nm (~5200 wavenumbers) which involve bending motions (Figure 4). Muscovite mica contains only OH^- groups and no molecular H_2O, so the bending vibration should be absent. This is frequently most readily verified in the 1900-nm region (Figure 5) because of interference from silicate absorption in the 1600-wavenumber region when thick samples are examined. The presence or absence of the bending-related absorptions is the primary distinction between the two major hydrogen species, H_2O and OH.

Water commonly exists in minerals as fluid inclusions. To distinguish fluid water from crystallographically bound water, spectra are obtained at cryogenic temperatures. Figure 6 compares the IR spectrum of water and ice in an artificial "fluid inclusion" formed by sandwiching water between two Al_2O_3 windows. The 78 K spectrum demonstrates the utility of low temperature measurement in identifying hydrogen as fluid inclusions. The band at 3200 wave-

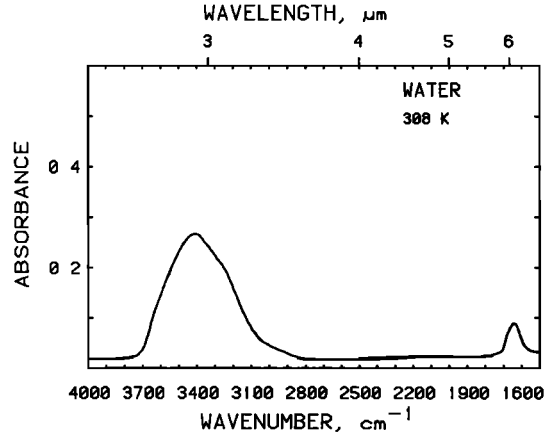

Fig. 1. Infrared absorption spectrum of a film (~1 μm thick) of liquid water showing the the overlapping stretching modes near 3400 wavenumbers and the bending mode near 1630 wavenumbers.

numbers that forms at 78 K is characteristic of ice [Eisenberg and Kauzmann, 1962, Chap. 3].

Case Studies

H_2O in Cordierite and Beryl

Beryl and cordierite have structures consisting of sixfold rings of silicate tetrahedra joined by other octahedrally and tetrahedrally coordinated cations in such a way that open channels exist parallel to the c axis. Both minerals also commonly yield H_2O upon analysis. Schreyer and Yoder [1964] demonstrated that the hydrogen speciation in cordierite was, in fact, as H_2O and that it resided in the channels. Wood and Nassau [1967] showed that the hydrogen speciation in beryl was also as H_2O and showed from the polarization dependence of the absorption that it occupied two distinct sites.

Absorption of light by an O-H bond occurs when the electric vector of the light is oriented parallel to the direction of the dipole. When more than one O-H is involved in absorbing the light, symmetry considerations determine the

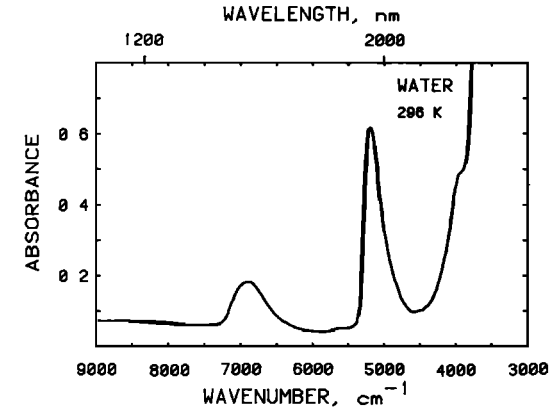

Fig. 2. Near-infrared absorption spectrum of film (100 μm thick) of liquid water showing the the first O-H stretching overtone near 7000 wavenumbers and the stretch plus bend combination mode near 5000 wavenumbers.

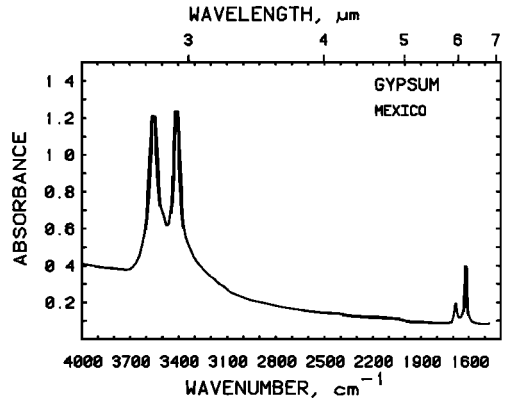

Fig. 3. IR spectrum of 0.50 mg powdered gypsum in a KBr pellet showing the separation between the two O-H stretching modes near 3500 wavenumbers and the bending modes of H_2O near 1600 cm^{-1}.

directions in which light is absorbed. In order to understand the spectrum of H_2O in beryl and cordierite, we first consider the detailed nature of the IR absorption of isolated H_2O molecules.

Figure 7 shows schematically the type of motion constituting the vibrations of H_2O. There are three atoms in the molecule, and therefore the motions of these atoms have 3x3 = 9 degrees of freedom. Three of these are translations of the entire molecule ($T_{x,y,z}$) and three are rotations of the entire molecule ($R_{x,y,z}$) around mutually perpendicular axes. This leaves 3 degrees of freedom representing internal vibrations of the molecule, where the atoms move relative to each other. These three vibrations are labeled ν_1, ν_2, and ν_3. They are the symmetric stretching, bending, and asymmetric stretching, respectively, of the H_2O molecule. Group theory shows that ν_1 and ν_2 occur when the incident light is polarized in the direction of the twofold symmetry axis of the H_2O molecule, and ν_3 occurs when the incident light is perpendicular to this direction but in the plane of the molecule. The most intense absorption bands of H_2O

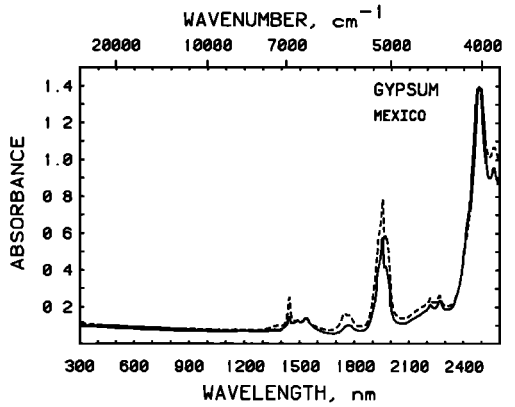

Fig. 4. Near-IR spectrum of a 0.34-mm-thick cleavage plate of gypsum showing overtone and combination modes, including the mode near 5000 wavenumbers (1900 nm) which is caused by the molecule H_2O. Taken with light polarized in the optical X (dashed line) and Z (solid line) direction.

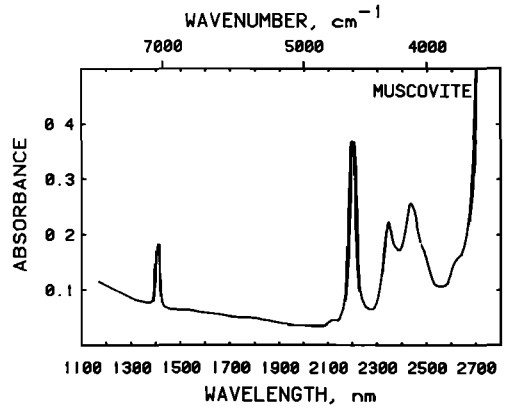

Fig. 5. Unpolarized NIR spectrum of a cleavage plate of muscovite showing the overtone of the O-H stretch near 1400 nm and the absence of an H_2O combination mode near 1900 nm. Thickness = 0.25 mm; sample oriented 45° to the incident beam.

are the fundamentals. The combination modes have very low intensity. It is also possible for bands which are "not allowed" by symmetry to have a small but observable intensity due to limitations in the assumptions used to calculate selection rules.

Wood and Nassau determined that there are two distinct groups of bands in the beryl spectrum that vary according to the chemistry of the sample. From the polarization behavior of these groups of bands, they were able to deduce that one type of molecule is oriented with the H-H vector parallel to c, and that the other H_2O molecule is oriented with its H-H vector perpendicular to the c axis.

Goldman et al. [1977] demonstrated that a similar situation exists in cordierite. In both minerals the frequencies of the absorptions (Figure 8) occur at lower energies than in the vapor H_2O, indicating that interaction occurs with the other constituents of the mineral. However, the shifts are not great, and the close correlations with the spectrum of water vapor, the sharpness of the bands, and the presence of bands identified as rotation plus vibration indicate that the H_2O molecules in beryl and cordierite are only weakly hydrogen bonded.

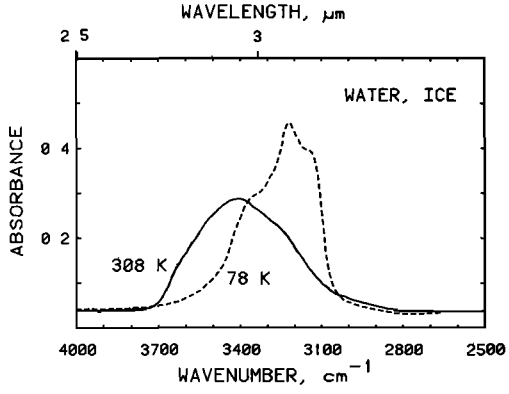

Fig. 6. Comparison of the infrared spectra of a thin film (~1 μm thick) of liquid water (solid line) to the same thickness of ice at 78 K (dashed line).

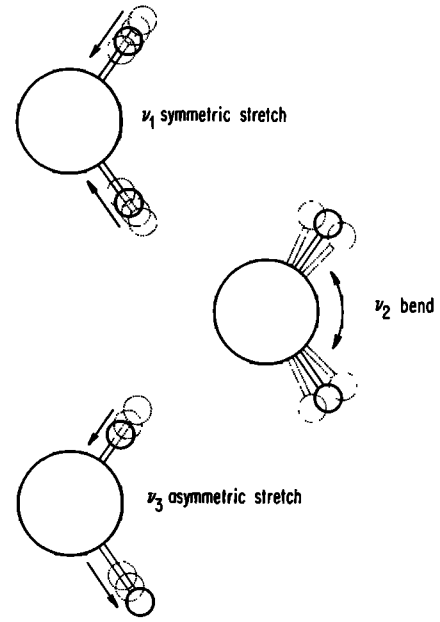

Fig. 7. Modes of vibration of the H_2O molecule.

Hydrogen in Quartz

Quartz is the most extensively studied natural system containing trace hydrogen. Hydrogen is ubiquitous in quartz, usually at levels of tens to hundreds of ppm. The most important tool in this field of study has been IR spectroscopy due to its sensitivity to the O-H bond.

Figure 9 shows the spectrum of a natural, clear quartz taken at 78 K. Most quartz spectra show a complexity of sharp peaks at low temperature. Figures 10 and 11 are the spectra of a natural amethyst crystal measured at room temperature and 78 K. The broad band (near 3400 wavenumbers) superimposed upon the sharp band spectrum is characteristic of synthetic quartz and natural quartzes formed at low temperatures [Frondel, 1982]. These two spectra exemplify the two important classes of absorption spectra in the quartz IR spectrum: sharp band absorption and broad band absorption.

Kats [1962] conclusively showed that the sharp band absorptions are due to O-H stretching vibrations. In a study that remains the classic work in the field, Kats showed that the great variety

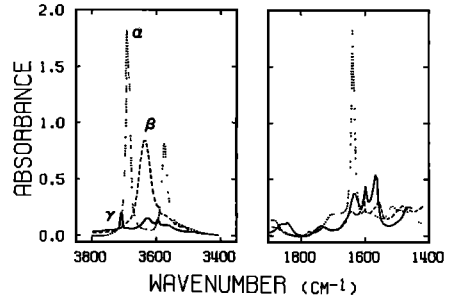

Fig. 8. IR spectrum of water in cordierite. The spectrum, taken in polarized light, shows more than two features in the 3600-wavenumber region because water occurs in more than one site [from Goldman et al., 1977, Figure 7].

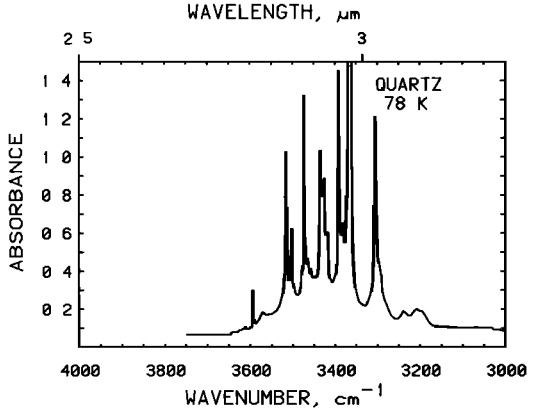

Fig. 9. IR spectrum of a 5-mm-thick natural Brazilian quartz crystal showing the complexity of the O-H stretching region. Sample temperature, 78 K, polarized perpendicular to c.

of absorptions are primarily due to the presence of Al^{3+} substitution for Si^{4+} and coupled charge-balancing alkali cations as well as other alkali cation defects in the crystal. Table 1 summarizes Kats' results and his peak assignments as well as additions that have been made by subsequent workers. Despite the assignment of 57 peaks in this table, this is still not a complete description of the quartz O-H vibrational spectrum.

The major tools used by Kats and later workers to index these peaks are electrolytic exchange and high-temperature diffusion. Kats obtained the data in Table 1 by exchanging Na^+, K^+, Li^+, Ag^+, and Cu^+ into clear, natural quartz crystals. He verified that the resulting absorptions were due to hydrogen defects by duplicating all the cationic exchanges under conditions where deuterium defects were formed. Three types of defects may be distinguished: (1) those in which alkali and hydrogen ions are associated, (2) defects involving two or more hydrogens, and (3) associations of aluminum-hydrogen.

Aluminum-hydrogen defects are the most stable type, persisting to over 1200°C at 1 atm. Kats distinguishes three major Al(H) peaks at 3310, 3374, and 3440 wavenumbers. They are all due to H^+ occurring in a charge-compensating role for Al^{3+} in an Si^{4+} site. They are stable at high temperatures because they are an intrinsic part of the crystal structure. These centers can be destroyed by intense electrolysis in a vacuum, resulting in oxygen vacancies forming the charge compensation for Al^{3+} [Kats, 1962; Krefft, 1975]. Kats demonstrates that there are two important Al(H) defects in quartz, one giving rise to the 3310-wavenumber peak and one giving rise to the 3370,3345-wavenumber pair. They are separate defects since the intensities of their infrared absorptions vary independently. He concludes, based largely on the orientation of the O-H vectors in these defects, that the 3310-wavenumber peak arises from H^+ bound between the two nonequivalent oxygens in an aluminum tetrahedron and that the 3370,3345-wavenumber pair arises from an hydroxide in the aluminum tetrahedron with the O-H vector pointing into the c axis "channel," making an angle of 75° with the c axis.

Much less can be said about the structure of the alkali-hydrogen and hydrogen-hydrogen defects. The overall stoichiometry of these defects is neutral, since they can be entirely removed and reintroduced by electrolysis. This suggests overall stoichiometries such as LiOH and HOH. The occurrence of new peaks when hydrogen is exchanged into the crystal suggests reactions such as LiOH to HOH, but any number of other geometries could be proposed where the introduced H^+ perturbs another O-H group without being directly bonded to it. Kats is of the opinion that several of the hydrogen defect bands are due to H_2O based largely on the greater width of the bands compared to the other sharp bands (Table 1). However, the characteristic overtone at 1900 nm due to bending and simultaneous stretching of an H_2O molecule has not been correlated with these IR bands and probably cannot be due to low intensity.

There are associations in the alkali defect data indicating that several classes of defects occur. For instance, the peaks at 3396(Li^+), 3382(Na^+), and 3354(Ag^+) have identical shifts upon deuteration, suggesting that they have the same structure. The Li(H) peaks at 3520 and 3396 wavenumbers always behave together and are independent of the Li(H) peaks at 3478 and

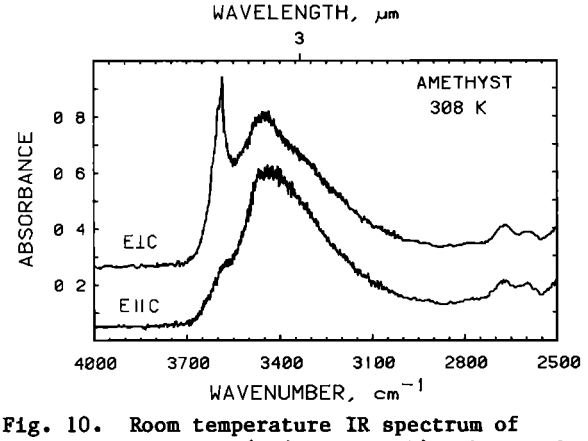

Fig. 10. Room temperature IR spectrum of Brazilian amethyst (1.41 mm thick) taken with polarized light vibrating perpendicular to c axis (upper trace) and parallel to c (lower trace).

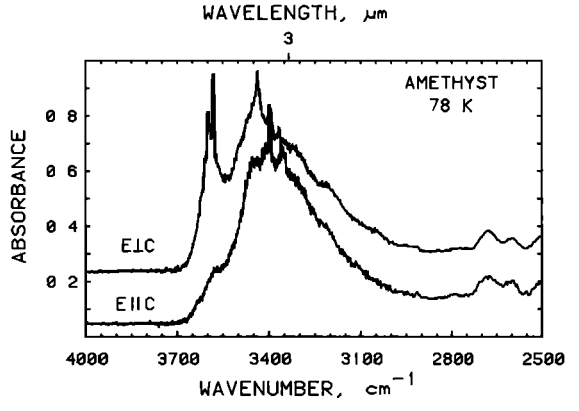

Fig. 11. Low-temperature IR spectrum of the sample whose spectrum appears in Figure 10.

3440 wavenumbers. The second pair are also stable to higher temperatures. Chakraborty and Lehmann [1976a] conclude, based on orientation of O-H vectors, that there are no molecules of the type LiOH existing in the c axis channels of quartz, the most logical opening in the structure. A number of plausible structures for defects in quartz have been proposed [Kats, 1962; Kirby, 1984; Chakraborty and Lehmann, 1976b], but the actual structures are still not known.

Hydrogen in Low-Temperature Quartz. Amethyst, chalcedony, opal, citrine, and synthetic quartz are all characterized by IR spectra in the O-H stretching region showing a broad band with superimposed sharp bands. While there are substantial differences in their IR spectra, the similarities merit discussing them simultaneously.

In some cases, the sharp bands in these low-temperature silicas are almost certainly due to the same factors discussed previously. For instance, Hosaka and Taki [1981a, b, c, d] report an intense band at 3450 wavenumbers in a synthetic quartz grown in NaCl solution. This band is probably the same band reported by Kats as the most intense natural quartz Na(H) band, at 3453 wavenumbers (Table 1). The shift may be due to instrumental calibration. Hosaka and Taki also consistently find bands at 3364 and 3304 wavenumbers in quartz grown in NaCl, KCl and pure water solutions. These correlate with Kats' Al(H) defects. (The source of aluminum is the source quartz material.) Koop and Staats [1970] also report these bands for synthetic quartz; Chakraborty and Lehmann [1978] report bands in these positions and with similar intensities for synthetic quartz and citrine. They are absent from chalcedony [Frondel, 1982] and at least some amethyst [Chakraborty and Lehmann, 1976a]. Frondel suggests that this is due to the low Al content of low-temperature natural quartz.

Aside from these instances, there is little correlation between the sharp bands in low-temperature quartzes and their trace constituents. Many authors [e.g., Kats 1962; Koop and Staats, 1970] cite this lack of correlation. Koop and Staats succeeded in growing Rb-doped quartz but observed no new peaks as a result of an RbOH component. They confirmed a result of Kats which is crucial to understanding synthetic quartz. In a wide range of synthetic crystals doped with alkalies and other monovalent impurities, the sum of the molar concentrations of monovalent cations is approximately equal to the concentration of Al^{3+}. It appears that all the alkalies are involved in charge compensation for aluminum and cannot compensate for OH groups, so alkali hydrogen defects cannot form. Hosaka and Taki show that Al(H) centers are allowed by an excess of Al^{3+} over alkalies in their crystals.

We are left with two types of unexplained absorption in low-temperature quartzes: the majority of the sharp band absorptions and the characteristic broad band absorption, which is correlated with a variety of physical properties. The nature of the broad band absorption is of substantial economic and scientific interest. Many structures and mechanisms of formation have been proposed for the hydrogen defect(s) responsible for the broad band absorption (see Kirby [1984] for a review). The outstanding problem is to establish which structures are consistent with the observed spectra.

Kats established that the broad band in synthetic quartz is related to hydrogen impurity by observing the spectrum of quartz grown in D_2O. Calibration curves now exist [Kirby, 1984] relating the total hydrogen content of synthetic quartz to the intensity of this band. The concentration of hydrogen in synthetic quartz is known to increase with growth rate, along with the concentration of other impurites [Frondel, 1982; Barnes et al., 1976]. The concentration decreases with increasing growth temperature, suggesting that the broad band in natural low-temperature quartz has a similar origin and that its absence in pegmatitic quartz such as that commonly obtained from Brazil is due to the higher growth temperature of such quartz.

Frondel [1982] studied the IR spectra of chalcedony and determined that the majority of its hydrogen is contained in two major species: surface hydroxyl groups and water molecules hydrogen bonded to those surface hydroxyls. The similarities between the behavior of chalcedony and synthetic fumed silica [McDonald, 1956] were used by Frondel to make these assignments. The adsorbed water appears to be responsible for the broad band absorption and the hydroxyls for the sharp bands. When chalcedony is heated, a sharp band appears at 3744 wavenumbers. By analogy to fumed silica, Frondel assigns this to nonhydrogen-bonded surface hydroxyl. Frondel notes that in geodes, crystalline α-quartz growing on chalcedony has a spectrum similar to the chalcedony in the O-H region, which is also the spectrum found in other low-temperature quartz such as amethyst and synthetic. These are not fibrous, so the fumed silica analogy is not entirely applicable unless the c axis "channels" are capable of creating a similar situation. No band above 3700 wavenumbers has been reported in crystalline α-quartz. Flörke et al. [1982] studied the NIR spectra of several types of fibrous and microcrystalline natural silicas. The major hydrogen species in them was found to be water, interpreted as liquid water between grains and fibers.

Figure 12 shows the IR spectrum of a typical synthetic quartz. The spectrum does not change substantially when the sample is cooled to 78 K. Figure 13 is a typical NIR spectrum of synthetic quartz. This spectrum is dominated by the 1920 nm (bend plus stretch) band for molecular H_2O (R.D. Aines et al., manuscript in preparation, 1983). There is a minor absorption in the 2250-nm region due to (bend plus stretch) of SiOH groups. Molecular H_2O appears to be the dominant speciation for the hydrogen in synthetic quartz. The spectra of natural amethyst (Figures 10 and 14) are very similar to that of synthetic quartz (Figures 12 and 13). The major difference between the synthetic quartz and the amethyst shown here is in the SiOH region; SiOH is the dominant hydrogen defect in this amethyst.

Opals may contain up to 8 wt % "H_2O." In the near-infrared spectra of opals, Langer and Flörke [1974] recognized the presence of both molecular water and SiOH groups. The 1900-nm region of the 296 K opal spectrum (Figure 15) shows two overlapping components. Langer and Flörke assigned

the sharper, higher-energy absorption to isolated water molecules encased in the silica structure and the broader one at 1957 nm to liquidlike, hydrogen-bonded water. The absorption at 2220 nm was assigned to SiOH groups in the silica which were not interacting with other H_2O groups, whereas the absorption at 2260 nm was assigned to SiOH groups at the interface with the water-like H_2O and which are hydrogen bonded to the H_2O.

The spectrum of opal taken at 78 K shows substantial peak shifts for Langer and Flörke's liquidlike water. This is consistent with the formation of ice. Figures 16 and 17 show the IR and NIR spectra of milky quartz. Here there is very similar behavior upon freezing. The fluid inclusions in this sample and the liquidlike water in opal represent large agglomerations of water molecules that are spectroscopically distinct from the nonfreezable water molecules in opal, amethyst, and synthetic quartz.

Summary: Proposed hydrogen defects in low-temperature quartz. Kirby [1984] discusses a number of mechanisms proposed for the incorporation of hydrogen in synthetic quartz. Two mechanisms that he favors are substitution of an $H_4O_4^{4-}$ group for SiO_4^{4-} (the hydrogarnet substitution) and a model involving chains of OH groups. The second model would result in a broad band absorption due to interactions among the OH groups through hydrogen bonds in the following

TABLE 1. Peak Assignments for O-H Stretch in Quartz

Peak Location at 78 K[a] cm^{-1}	Assigment or Observed Association[b]	Intensity Relative to Associated Peaks[c]	Method of Assignment[d]	Comments: Type of Quartz Where Found[e]	Reference[f]
3610	K^+	k = 6	A.E.	natural clear	1
3600	?	α = 0.1	—	synthetic	1
3590	H^+	α = 0.5	A.E	natural clear	1
3585	K^+	k = 4	A.E	natural clear	1
3585	?	α = 1.3	—	synthetic, amethyst	1,2
3578	K^+	k = 6	A.E.	natural clear	1
3573	$Li^+ + \gamma$	α = 1.0	X ray	natural clear[g]	1
3567	K^+	k = 4	A.E.	natural clear	1
3556	Na^+	k = 8	A.E.	natural clear	1
3553	$Cu^+ + \gamma$	—	X ray	natural clear	1
3551	$Ag^+ + \gamma$	—	X ray	natural clear	1
3550	K^+	k = 7	A.E.	natural clear	1
3546	$Na^+ + \gamma$	—	X ray	natural clear	1
3540	Cu^+	k = 15	A.E.	natural clear	1
3535	Ag^+	k = 8	A.E.	natural clear	1
3538	K^+	k = 12	A.E.	natural clear	1
3534	Na^+	k = 12	A.E.	natural clear	1
3530	H^+	α = 0.5	A.E.	natural clear	1
3524	Ag^+	k = 7	A.E.	natural clear	1
3520 [3517]	Li^+	k = 30	A.E.	natural clear	1
3514	Cu^+	k = 12	A.E.	natural clear	1
3513	Na^+	k = 18	A.E.	natural clear	1
3510 [3510]	Li^+	k = 14	A.E.	natural clear	1
3500	Ag^+	k = 6	A.E.	natural clear	1
3485	H^+	α = 1.0	A.E.	natural clear	1
3478 [3485]	Li^+	k = 17	A.E.	natural clear	1
3470 [3474]	?	α = 0.5	nat.	h	1,3
3462	Cu^+	k = 9	A.E.	natural clear	1
3462	H^+	α = 0.5	A.E.	natural clear	1
3460	K^+	k = 12	A.E.	natural clear	1
3454	Ag^+	k = 7	A.E.	natural clear	1
3453	Na^+	k = 48	A.E.	natural clear	1
3440	i	α = 0.5	—	synthetic, amethyst	1,2
3440 [3443]	Li^+	k = 15	A.E.	natural clear	1
3435 [3432]	Al^{3+}	α = 1.5	nat.	Fermi pair with 3373[j]	1
3422	H^+	α = 0.5	A.E.	natural clear	1
3415	Cu^+	k = 8	A.E.	natural clear	1
3414	K^+	k = 7	A.E.	natural clear	1
3408	$Li^+ + \gamma$	weak	X ray	>2 Mrads[k]	1
3400	H^+	α = 0.5	A.E.	natural clear	1
3400	Ag^+	k = 9	A.E.	natural clear	1
3400	Na^+	k = 7	A.E.	natural clear	1
3400	i	α = 0.3	—	synthetic, amethyst	1
3396 [3405]	Li^+	k = 36	A.E.	natural clear	1
3382	Na^+	k = 42	A.E.	natural clear	1

TABLE 1. (continued)

Peak Location at 78 K[a] cm^{-1}	Assigment or Observed Association[b]	Intensity Relative to Associated Peaks[c]	Method of Assignment[d]	Comments: Type of Quartz Where Found[e]	Reference[f]
3380	?	weak	nat.	natural clear	1
3375	?	medium	nat.	amethyst	1,2
3371 [3383]	Al^{3+}	α = 9.0	nat.	Fermi pair with 3435[j]	1
3365	?	α = 0.2	—	synthetic	1
3355	i	α = 0.3	—	synthetic, amethyst	1,3
3310 [3318]	Al^{3+}	α = 3.0	nat.	natural clear	1
3305	H^+	α = 0.5	A.E.	natural clear	1
3240	H_2O	weak	A.E.	very broad[ℓ]	1
3222	H_2O	weak	A.E.	very broad[ℓ]	1
3205	?	weak	nat.	natural clear	1

[a]Peak locations measured at 78 K by Kats [1962]; room temperature values in brackets where available.

[b]Most assignments by Kats; (+ γ) means after irradiation of alkali exchanged material; '?' where peak is reported in literature but not assigned or assigned with doubts by the authors.

[c]Intensities from Kats. These should only be used to compare like associations, for instance, comparing one Cu^+ peak to another. k is the integral absorbance per 10^{-2} m; α is the absorbance per 10^{-2} m.

[d]Usually alkali exchange (A.E.) and deuteration by Kats. Dashes indicate where not assigned. 'nat.' where assigned on the basis of occurrence in natural material and other criteria without alkali exchange.

[e]Type of quartz listed as "natural clear" when that is what Kats used to make initial assignment. Many of these peaks also occur in amethyst and synthetic quartz.

[f]References: 1, Kats [1962]; 2, Chakraborty and Lehmann [1976a]; 3, Krefft [1975]; 4, Chakraborty and Lehmann [1978].

[g]Observed only in clear samples that color yellow upon irradiation and not in those coloring brown. Peak disappears if dose exceeds 5 Mrads.

[h]This band was observed by Kats to persist above 1000°C, along with bands assigned to Al^{3+}. Krefft [1975] produced this band by prolonged electrolysis in H_2O or H_2 atmosphere; it was accompanied by a yellow coloration in the sample.

[i]Chakraborty and Lehmann [1976a] assign these bands to "H^- bonded directly to Si." However, later papers by the same authors make no mention of this assignment.

[j]These peaks are assigned by Kats as due to H^+ in a charge compensating role for Al^{3+} substitution for Si^{4+}. They are stable to above 1000°C, unlike all the other peaks in this table. The peaks at 3435 and 3373 are a fermi resonance pair formed by a lattice mode and an O-H mode at about 3410.

[k]Occurs in quartz coloring yellow by irradiation, as in footnote g but only after dose exceeds 2 Mrads.

[ℓ]Kats assignment of these bands is based on their breadth and the fact that they are formed at the expense of bands he interprets as due to LiOH under hydrogen exchange.

fashion:

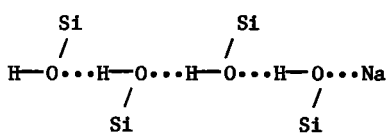

The spectroscopic features of $H_4O_4^{4-}$ are not well established experimentally. However, the hydrogarnet substitution does not yield an absorption at 1900 nm, since all the hydrogens are attached to different oxygens [Aines and Rossman, 1982]. In fact, the presence of molecular H_2O as indicated by the 1920-nm band in synthetic quartz indicates that neither proposed substitution is the major hydrogen defect in synthetic quartz. However, the minor absorptions at 2250 nm (Figure 13) could be due to these substitutions.

Effect of water on the properties of quartz. The effect of water on the mechanical properties of quartz is well known and is the subject of several papers in this volume. Water also has a strong correlation with radiation damage in quartz. The most spectacular form of radiation damage in quartz is the removal of an electron from a substitutional Fe^{3+} to yield Fe^{4+} and amethyst [Cox, 1977]. No change in the O-H vibrational spectrum accompanies this oxidation, and no Fe^{3+}(H) defect has been identified analagous to the Al(H) defects [Chakraborty and Lehmann, 1978]. However, other changes in the O-H spectrum are associated with radiation damage in quartz. These are interesting in terms of understanding both the nature of hydrogen defects

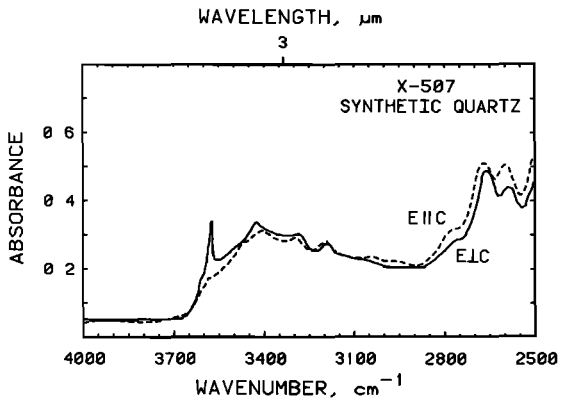

Fig. 12. Room temperature IR spectrum of synthetic quartz. Sample 3.97 mm thick. Dashed trace polarized parallel to c, solid trace perpendicular to c. From block E of crystal X-507.

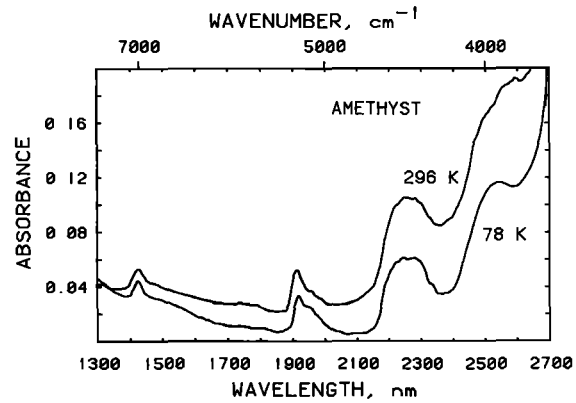

Fig. 14. Unpolarized NIR spectra of Brazilian amethyst, 5.72 mm thick. Upper trace room temperature; lower trace cooled to 78 K.

and radiation damage mechanisms in quartz.

Kats [1962] performed radiation experiments on synthetic and natural clear quartz. Two effects are noted on the IR spectrum. Associated with each cation is at least one new band that forms upon irradiation (Table 1). Also, the intensity of the bands assigned to Al(H) defects increase in natural quartz at the expense of the prevalent alkali-hydrogen defect. In synthetic quartz, the bands assigned to Al(H) defects grow, sometimes with accompanying decrease of other sharp bands. These results are in agreement with current thought about the nature of radiation damage to Al(H) and Al(alkali) defects obtained from other methods reviewed by Weil [1975]. The common manifestation of radiation damage of this kind is the formation of smoky coloration [Weil, 1975] due to the presence of $[AlO_4]^{4-}$ centers. They are formed by the removal of an electron and an alkali ion from the vicinity of the aluminum tetrahedron. This can be duplicated by electrolysis in vacuum [Krefft, 1975]. When such a crystal is heated, the alkali diffuses back and destroys the color center. Al(H) defects do not form smoky centers when irradiated at room temperature, apparently because the proton can diffuse back too easily. When irradiated and observed at 78 K [Mackey, 1963], smoky centers form which are destroyed upon warming.

The effects of radiation on the IR spectrum of quartz may largely be explained by the mechanism just discussed. The growth of Al(H) absorptions at the expense of other absorptions is accordingly due to alkalies being removed from their charge-compensating position around an Al tetrahedron, but an H^+ diffuses to that site making an Al(H) defect. Presumably, an alkali-alkali defect is also formed which may have a spectroscopic manifestation if it is a complex one with hydrogen. However, the new alkali-hydrogen defects that arise upon irradiation could have many origins. One possible origin in synthetic quartz arises from a mechanism as follows: ionizing radiation dissociates an HOH group, giving neutral H and OH, which interact with an Al-alkali defect, giving an Al(H) defect and an alkali-hydrogen defect. Hosaka and Taki [1981d] noted that in quartz crystals grown from increasingly pure solutions, i.e., NaCl solution and pure water, the pure water-grown crystal showed essentially no radiation change, while the NaCl-grown crystal showed changes of the type discussed above.

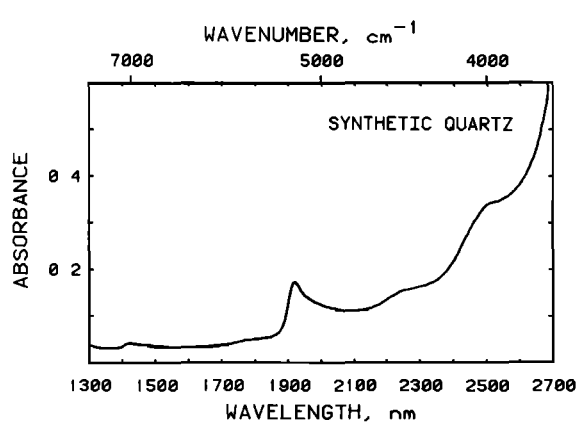

Fig. 13. Room temperature NIR spectrum of synthetic quartz X-13, 47.5 mm thick, showing the molecular H_2O band near 1900 nm. Taken with light polarized parallel to c axis. The perpendicular spectrum has an additional peak at 2215 nm of absorbance 0.01 but is otherwise identical.

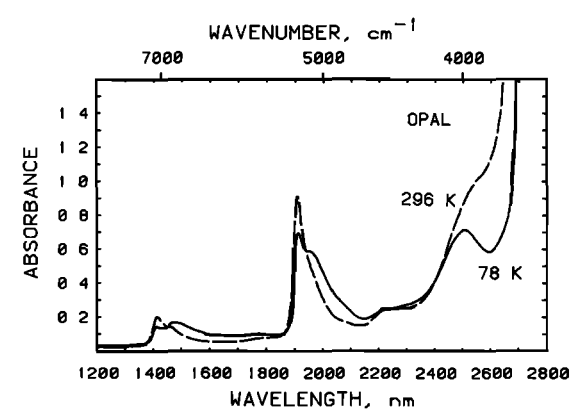

Fig. 15. NIR spectrum of an opal from Opal Mountain, San Bernardino County, California, 1.288 mm thick. Solid line 78 K; dashed line 296 K. The molecular H_2O bands at 1900 nm are prominent.

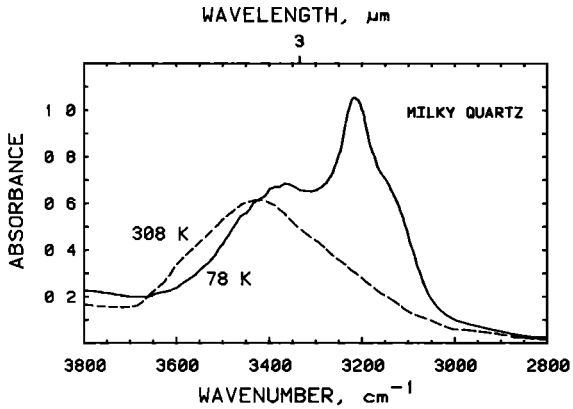

Fig. 16. IR spectrum of milky quartz from Dillsburg, Pennsylvania, 1 mm thick, showing water bands at 308 K (dashed line) and ice bands at 78 K (solid line).

The association of water speciation with a physical property of quartz is well illustrated by Figures 18 and 19. They show the spectra of two zones of different color in a single quartz crystal zoned with both the amethyst and citrine color varieties. The broad band in the spectrum of the citrine zone is due to molecular H_2O similar to that in synthetic quartz. The amethyst zone in this crystal has only sharp band absorption in its spectrum indicative of OH^- ions. Whether water inhibits amethyst formation, promotes citrine formation, or is coincidentally associated with another substituent cannot be determined from these data alone. However, Maschemeyer et al. [1980] have proposed, based on EPR evidence, that the citrine color center is composed of a Li-Al smoky-type hole center, adjacent to a silicon vacancy. They suggest that one way to generate such a vacancy is by incorporating H_2O in the Si site, with adjacent Si atoms moving to interstitial sites to minimize charge imbalance.

Spectroscopy of Fluid Inclusions

Fluid inclusions are an important site for hydrogen in minerals. In principle, there should

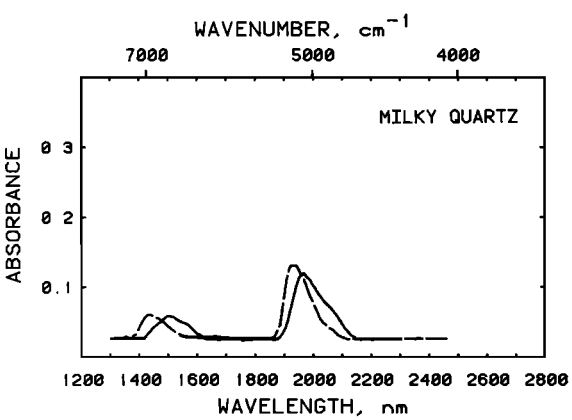

Fig. 17. NIR spectrum of milky quartz from Dillsburg, Pennsylvania, at 296 K (dashed line) and 78 K (solid line) showing ice bands. A sloping baseline due to scattering has been subtracted out. Thickness = 3 mm.

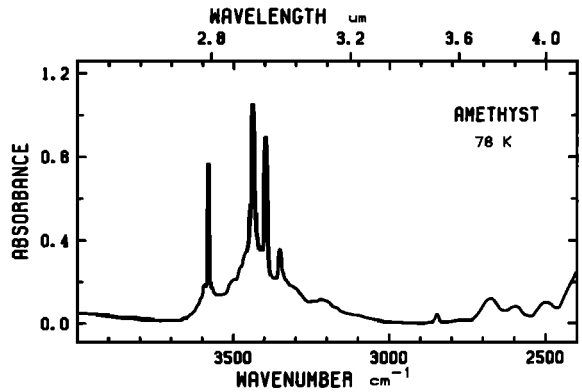

Fig. 18. IR spectrum of zoned amethyst-citrine in the amethyst zone showing absorption from OH ions, 78 K, 2 mm thick.

exist a continuum between an isolated water molecule and a large fluid inclusion containing millions of water molecules. It would be desirable to differentiate between single water molecules, small clusters of water molecules that are crystallographically constrained, and "bulk" water in fluid inclusions of the classical definition.

We have already discussed some examples (cordierite, gypsum) of the spectroscopic behavior of isolated water molecules in a crystal structure. An interesting model system for small groups of water molecules was studied by Van Thiel et al. [1957]. They froze varying concentrations of H_2O in an argon matrix at 8 K, creating "pockets" containing varying numbers of H_2O molecules. In this system, the pockets are expected to be completely "filled" by H_2O; that is, the matrix conforms to the H_2O it entraps. This system should be a reasonable model for H_2O trapped in a locally neutral silicate lattice. No attempt was made to characterize directly the shapes and sizes of the entrapping volumes.

Van Thiel et al. recognized four polymeric species of H_2O. Their assignments of the IR absorption patterns are given in Table 2. The assignments for the tetramer are tentative because of the spectral complexity at high H_2O concentrations. In the bending region the formation of higher polymers resulted in a shift of complex absorptions toward 1650 wavenumbers from the monomer frequency of 1595 wavenumbers; the

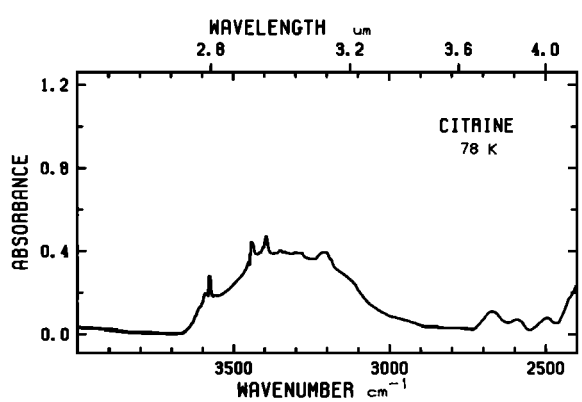

Fig. 19. IR spectrum of zoned amethyst-citrine in the citrine zone showing the broad band absorption from H_2O molecules, 78 K, 2 mm thick.

TABLE 2. Vibrational Bands for Polymeric Water Species Entrapped in Solid Argon Matrix

Polymeric Species	Stretching Frequency ν_{OH}, cm^{-1}
Monomer	3725 , 3627
Dimer	3691 , 3546
Trimer	3510 , 3355
Tetramer	3318?, 3322?

From Van Thiel et al. [1957].

actual peaks could not be assigned for the polymeric species in the bending region. As the concentration was raised to the point where tetramers and higher polymers predominated, the O-H stretch region was dominated by a broad band in the 3400- to 3200-wavenumber region. This study suggests what type of behavior should be expected from small groups of H_2O molecules in a mineral such as quartz. Interestingly, as the H_2O concentration increases, the total integrated absorption increases nonlinearly. The ε value increases sharply as more H_2O is bound in polymers where hydrogen bonding occurs. This is in accord with Paterson's [1982] appraisal of ε values in minerals and glasses.

The next model system to be considered is one in which the water molecules are coordinated directly or indirectly to a cation, providing a contrast to the neutral argon matrix. Clays such as hectorite contain exchangable Na^+ or Mg^{2+} between layers formed by silicate tetrahedra and octahedra of other cations. The interlayer cations serve to balance charge deficiencies within the layers, but in contrast to the otherwise similar cations in micas, these cations will readily become hydrated by up to 24 water molecules [Farmer and Russell, 1971].

Hectorite can exist in three states of hydration: completely hydrated with multiple H_2O per cation, trihydrated, and monohydrated. The fully hydrated form is characterized by a broad band absorption centered at 3370 wavenumbers and a sharper band superimposed at slightly higher frequencies. Farmer and Russell interpret this spectrum and the spectra of the partially deuterated clays as being due to extended chains of water molecules in the fully hydrated forms extending from the cation to an oxygen adjoining the site of charge imbalance in the layer, i.e., for the fully deuterated form:

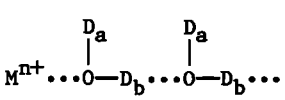

They state that the OD_a groups are mostly directed toward the oxygens of the silicate lattice and form weak hydrogen bonds with those surface oxygens which carry little or no charge. They give rise to the sharp band while the OD_b groups give rise to the broad band. Sharper, more resolved patterns were obtained for the lower hydrates.

A third model system is water in classic fluid inclusions. These are possible in all minerals and have been extensively studied. Kekulawala et al. [1981] studied fluid inclusions in synthetic quartz, integrating results from IR, TEM, and strain measurements. Hydrous synthetic quartz becomes cloudy if heated or strained. Kekulawala et al. demonstrated that this cloudiness is due to the precipation of the hydrogen in the sample into fluid inclusions. Once this occurs, the quartz behaves similarly to natural milky quartz, which has much higher ductility and Q value than synthetic quartz. These physical properties in synthetic quartz only correlate when the hydrogen is in some more dispersed form than fluid inclusions.

Figures 6 and 20 show the IR and NIR regions of an artificial "fluid inclusion" formed by sandwiching water between two Al_2O_3 windows. They are shown at room temperature and 78 K to demonstrate the utility of low-temperature measurement in identifying hydrogen in fluid inclusions. Kekulawala et al. [1981] discovered that the broad band absorption at 3400 wavenumbers does not disappear totally as the 3200-wavenumber band forms, as it does in pure ice [Eisenberg and Kauzmann, 1962]. This behavior is also seen in the spectra of the 2-μm-thick artificial inclusion and the milky quartz (Figures 6 and 16). They interpreted the persistence of this band as a result of the H_2O monolayer at the edge of the fluid inclusion. This water still in contact with the silicate lattice never attains the ice structure. They measured the diameters of the fluid inclusions by TEM and calculated the extent of the monolayer for a 60-nm inclusion at two internal pressures. At 180 MPa it would be 10% of the inclusion; at 50 MPa it would be 30%. It does not appear that IR spectroscopy can accurately identify extremely small fluid inclusions, given the current understanding of their behavior. All the H_2O would be involved in the monolayer; it would not form "ice" at low temperature. This limit may extend to hundreds of molecules in a cavity.

Before heat treatment, Kekulawala et al.'s sample contained small contrast features observed in TEM which they describe as having the "characteristics of sources of hydrostatic pressure." Heating diminishes their number, with an increase in the number of identifiable fluid inclusion bubbles. If these small contrast features are

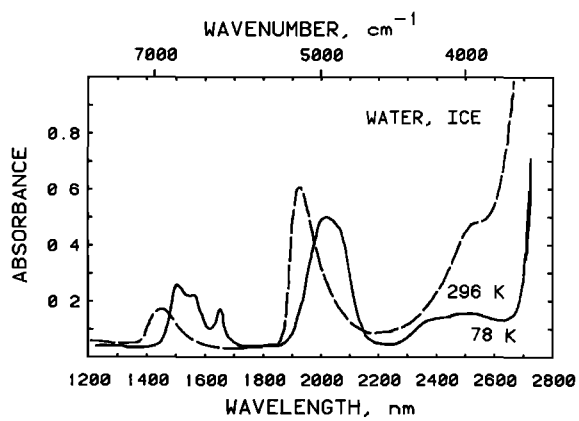

Fig. 20. NIR spectrum of water at 296 K (dashed line) and ice at 78 K (solid line). Sample 100 μm thick.

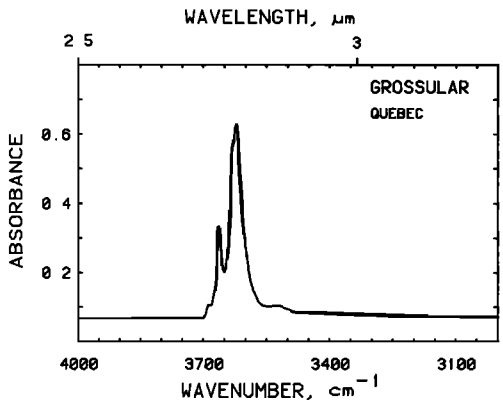

Fig. 21. IR spectrum of grossular garnet showing OH stretching absorptions. Sample 150 μm thick.

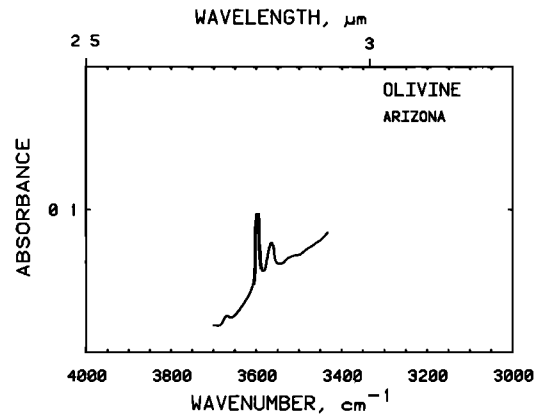

Fig. 22. IR spectrum of olivine showing O-H stretching absorptions. Sample 9.5 mm thick.

very small fluid inclusions, it is probable that they will not give the infrared spectrum of a fluid inclusion at 78 K because of the monolayer effect described above.

Trace "Water" in Other Minerals

Most minerals show OH absorption in their infrared spectrum. Usually, the amounts are low, but it is present even in gem quality crystals. Examples are shown in Figures 21-23. The crystallographic details of the location of this "water" have been established in only a few of the minerals [Beran, 1969, 1970, 1971; Beran and Zemann, 1969, 1971; Beran and Putnis, 1983; Wilkins and Sabine, 1973]. In many of these studies, spectroscopic results have been reported for only one crystal, so that it is not possible to distinguish between OH present in foreign phases from OH which is crystal chemically bound in the host phase. Studies in progress in our laboratory indicate that OH is a common substituent in garnet [Aines and Rossman, 1982] and that minor amounts of water are commonly found in feldspars [Solomon and Rossman, 1982]. In natural feldspars higher water content is associated with a greater extent of Al/Si ordering. Water in feldspar is also intimately associated with radiation damage processes which generate the colored amazonite variety of potassium feldspar [Hofmeister and Rossman, 1981].

Example of Concentration Determination

The concentration of molecular water in fluid inclusions in the milky quartz, whose spectrum is illustrated in Figure 16, can be estimated by the following procedure:

1. From the room temperature spectrum the absorbance of the ~3400-wavenumber band is determined. To correct for the sloping baseline (a result of wavelength-dependent scattering in the sample), a sloping straight-line baseline is connected to lower portions of the data trace at the left- and right-hand sides. From the spectrum the peak of the absorption at 3400 wavenumbers is read to be 0.50 absorbance units above the baseline.

2. The Beer's law relationship is defined as $A = \varepsilon \times p \times c$, where A is the absorbance from the spectrum (0.50 in this case), p is the optical path length through the sample (in 10^{-2} m), c is the concentration of the species of interest (in moles per liter), and ε is the molar absorptivity constant obtained from a standard substance. Using the ε value of this band for H_2O in liquid water, 81 ℓ/mol/10^{-2} m [Thompson, 1965], the following calculation gives the concentration:

$$0.50 = 81\ \ell/(10^{-2}\ \text{m})\text{mol} \times 0.0195 \times 10^{-2}\ \text{m} \times c$$

$$c = 0.317\ \text{mol}/\ell$$

3. The concentration can be converted to wt % as follows: From the density of quartz, 2.65, a sample weight of 2.65 kg/ℓ is obtained. The water content is

$$0.317\ \text{mol} \times 0.018\ \text{kg mol}^{-1} = 5.70 \times 10^{-3}\ \text{kg } H_2O$$

or

$$5.70 \times 10^{-3}\ \text{kg}/2.65\ \text{kg} \times 100 = 0.215\%\ H_2O$$

Two major difficulties in determing concentrations are the determination of appropriate ε values for all the different types of H_2O and OH which occur in minerals and dealing with spectra with several overlapping bands. Paterson [1982] surveys available calibrations for the IR determination of water in quartz, glasses, and related substances. He provides his tabulations

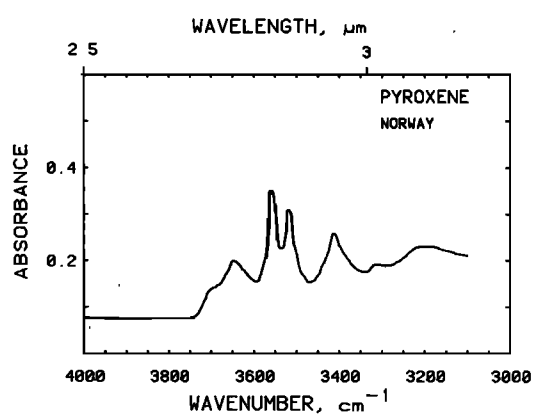

Fig. 23. IR spectrum of the orthopyroxene bronzite showing O-H stretching absorptions. Sample 410 μm thick.

in terms of integrated absorption profiles which have a smaller temperature dependence than ε values.

Acknowledgments. This work has benefited from discussions with Stephen Kirby (USGS), who also provided the synthetic quartz samples used in this study, and from Clifford Frondel (Harvard) who provided the results of his study of low temperature silica in advance of publication. This study was in part funded by the National Science Foundation (Grant EAR-7919987). Contribution 3832, Division of Geological and Planetary Sciences, California Institute of Technology.

References

Aines, R. D., and G. R. Rossman, The hydrous component in garnets (abstract), Geol. Soc. Am. Abstr. Programs, 14, 430, 1982.

Barnes, R. L., E. O. Kolb, R. A. Laudise, E. E. Simpson, and K. M. Kroupa, Production and perfection of z-face quartz, J. Cryst. Growth, 34, 189-197, 1976.

Beran, A., Über (OH)-Gruppen in Olivin, Anz. Oesterr. Akad. Wiss., Math. Naturwiss. Kl., 106, 73-74, 1969.

Beran, A., Messung des Ultrarot-Pleochroismus von Mineralen, IX, Der Pleochroismus der OH-Streckfrequenz in Titanit, Tschermaks Mineral. Petrogr. Mitt., 14, 1-5, 1970.

Beran, A., Messung des Ultrarot-Pleochroismus von Mineralen, XII, Der Pleochroismus der OH-Streckfrequenz in Disthen. Tschermaks Mineral. Petrogr. Mitt., 16, 129-135, 1971.

Beran, A., and A. Putnis, A model of the OH positions in olivine, derived from infrared-spectroscopic investigations, Phys. Chem. Miner., 9, 5760, 1983.

Beran, A., and J. Zemann, Messung des Ultrarot-Pleochroismus von Mineralen, VIII, Der Pleochroismus der OH-Streckfrequenz in Andalusit, Tschermaks Mineral. Petrog. Mitt., 13, 285-292, 1969.

Beran, A., and J. Zemann, Messung des Ultrarot-Pleochroismus von Mineralen. Der Pleochroismus der OH-Streckfrequenz in Rutil, Anatas, Brookit, und Cassiterit, Tschermaks Mineral. Petrogr. Mitt., 15, 71-80, 1971.

Chakraborty, D., and G. Lehmann, On the structures and orientations of hydrogen defects in natural and synthetic quartz crystals, Phys. Status Solidi A, 34, 467-474, 1976a.

Chakraborty, D., and G. Lehmann, Distribution of OH in synthetic and natural quartz crystals, J. Solid State Chem., 17, 305-311, 1976b.

Chakraborty, D., and G. Lehmann, On the fine structure in the infrared spectra of clear natural quartz, amethyst, citrine, and synthetic quartz crystals, Z. Naturforsch. A, 33, 290-293, 1978.

Cox, R. T., Optical absorption of the d^4 ion Fe^{4+} in pleochroic amethyst quartz, J. Phys. C, 10, 4631-4643, 1977.

Eisenberg, O., and W. Kauzmann, The Structure and Properties of Water, 296 pp. Oxford University Press, New York, 1962.

Farmer, V. C., and J. D. Russell, Interlayer complexes in layer silicates. The structure of water in lamellar ionic solutions, Trans. Faraday Soc., 67, 2737-2749, 1971.

Flörke, D. W., B. Köhler-Herbertz, K. Langer, and I. Törges, Water in microcrystalline quartz of volcanic origin: Agates, Contrib. Mineral. Petrog., 80, 329-333, 1982.

Frondel, C., Structural hydroxyl in chalcedony (Type B quartz), Am. Mineral., 67, 1248-1257, 1982.

Goldman, D. S., G. R. Rossman, and W. A. Dollase, Channel constituents in cordierite, Am. Mineral., 62, 1144-1157, 1977.

Hofmeister, A. M. and G. R. Rossman, Effects of radiation on water and lead in potassium feldspar (abstract), Geol. Soc. Am. Abstr. Programs, 13, 474, 1981.

Hosaka, M., and S. Taki, Hydrothermal growth of quartz crystals in NaCl solution, J. Cryst. Growth, 52, 837-842, 1981a.

Hosaka, M., and S. Taki, Hydrothermal growth of quartz crystals in KCl solution, J. Cryst. Growth, 53, 542-546, 1981b.

Hosaka, M., and S. Taki, Hydrothermal growth of quartz crystals in pure water, J. Cryst. Growth, 51, 640-642, 1981c.

Hosaka, M., and S. Taki, Synthetic quartz crystals grown in NaCl, KCl solutions and pure water, and their low temperature infrared absorption, Proc. Annu. Freq. Control Symp., 35, 304-311, 1981d.

Kats, A., Hydrogen in alpha quartz, Philips Res. Rep., 17, 133-195, 201-279, 1962.

Kekulawala, K. R. S. S., M. S. Paterson, and J. N. Boland, An experimental study of the role of water in quartz deformation, in Mechanical Behavior of Crustal Rocks, Geophys. Monogr. Ser., vol. 24, edited by N. L. Carter, pp. 49-60, AGU, Washington, D.C., 1981.

Kirby, S. H., Hydrogen-bonded hydroxyl in synthetic quartz: Analysis, mode of incorporation and role in hydrolytic weakening, Phys. Chem. Mineral., in press, 1984.

Koop, O. C., and P. A. Staats, Characterization of Rb-OH grown quartz by infrared and mass spectroscopy, J. Phys. Chem. Solids, 31, 2469-2476, 1970.

Krefft, G. B., Effects of high temperature electrolysis on the coloration characteristics and OH-absorption bands in alpha-quartz, Radiat. Eff., 26, 249-259, 1975.

Langer, K., and O. W. Flörke, Near infrared absorption spectra (4000-9000 cm^{-1}) of opals and the role of "water" in these $SiO_2 \cdot nH_2O$ minerals, Fortschr. Minereral., 52 (1), 17-51, 1974.

Mackey, J. H., Jr., EPR study of impurity-related color centers in germanium doped quartz, J. Chem. Phys., 39, 74-80, 1963.

Maschemeyer, D., K. Niemann, H. Hake, and G. Lehmann, Two modified smoky quartz centers in natural citrine, Phys. Chem. Miner., 6, 145-156, 1980.

McDonald, R. S., Study of the interaction between hydroxyl groups of Aerosil silica and adsorbed non-polar molecules by infrared spectrometry, J. Am. Chem. Soc., 79, 850-854, 1956.

Paterson, M., The determination of hydroxyl by infrared absorption in quartz, silicate glasses and similar materials, Bull. Mineral., 105, 20-29, 1982.

Schreyer, W., and H. S. Yoder, The system Mg-cordierite-H_2O and related rocks, Neues Jahrb. Mineral. Abh., 101, 271-342, 1964.

Solomon, G. C., and G. R. Rossman, Water in feldspars, (abstract), Geol. Soc. Am., Abstr. Programs, 14, 622, 1982.
Thompson, W. K., Infrared spectroscopic studies of aqueous systems, I, Trans. Faraday Soc., 61, 1635-1640, 1965.
Van Thiel, M., E. D. Becker, and G. C. Pimental, Infrared studies of hydrogen bonding by the matrix isolation technique, J. Chem. Phys., 27, 486-490, 1957.
Weil, J. A., The aluminum centers in α-quartz, Radiat. Eff., 26, 261-265, 1975.
Wilkins, R. W. T., and W. Sabine, Water content of some nominally anhydrous silicates, Am. Mineral., 58, 508-516, 1973.
Wood, D. L., and K. Nassau, Infrared spectra of foreign molecules in beryl, J. Chem. Phys., 47, 2220-2228, 1967.

R. D. Aines and G. R. Rossman, Division of Geological and Planetary Sciences, California Institute of Technology, Pasadena, CA 91125.

(Received October 13, 1982;
revised April 29, 1983;
accepted June 16, 1983.)